In situ EXAFS study of the bimetallic interaction in a rhenium-promoted alumina-supported cobalt Fischer–Tropsch catalyst

Magnus Rønning [a], David G. Nicholson [b] and Anders Holmen [a,*]

[a] *Department of Chemical Engineering, Norwegian University of Science and Technology (NTNU), N-7491 Trondheim, Norway*
E-mail: holmen@chembio.ntnu.no
[b] *Department of Chemistry, Norwegian University of Science and Technology (NTNU), N-7491 Trondheim, Norway*

Received 6 June 2000; accepted 25 January 2001

The local environments about the rhenium atoms in a Co–Re/γ-Al_2O_3 catalyst after different reduction periods have been studied by X-ray absorption spectroscopy (EXAFS). The bimetallic catalyst containing 4.6 wt% cobalt and 2 wt% rhenium has been compared with a corresponding monometallic sample with 2 wt% rhenium on the same support. The rhenium L_{III} EXAFS analysis shows that bimetallic particles are formed after reduction at 450 °C with the average particle size being less than 15 Å. More than 6 h reduction at 450 °C is required for complete reduction of accessible rhenium.

KEY WORDS: Fischer–Tropsch catalyst; bimetallic interaction; EXAFS; rhenium promoter; cobalt catalyst

1. Introduction

The Fischer–Tropsch synthesis has received much attention as a possible route in the synthesis of clean diesel fuel from natural gas. The route involves production of syngas from methane, Fischer–Tropsch synthesis of heavy waxes, and subsequent hydrocracking to clean middle distillates [1,2]. Cobalt-based bimetallic catalysts supported on Al_2O_3 [3–5] are often the preferred choice for the production of high molecular weight hydrocarbons from hydrogen-rich syngas [6]. This is due to the low water–gas shift activity of cobalt compared to, e.g., iron. The promoting metal (rhenium, ruthenium, palladium or platinum) appears to improve the dispersion of cobalt and hence increase the number of active sites. The nature of the cobalt metal phases on different supports has been extensively studied and is well established [7–13].

Structural studies on the state of the promoters are, however, relatively scarce. Iglesia et al. [8] reported bimetallic interaction between ruthenium and cobalt in an EXAFS/TEM study of bimetallic catalysts supported on TiO_2. Ruthenium was shown to be completely reduced and coordinated to approximately twelve metal atoms. The coordination towards cobalt increased with increasing calcination temperature. A recent study using EXAFS and XRD concluded that an alloy of palladium and cobalt is formed on palladium-promoted cobalt catalysts supported on graphite [14]. On the other hand, no clear evidence of alloy formation has been reported for the Co–Pt/Al_2O_3 catalyst system [15,16]. TPR studies of rhenium on alumina indicate that two rhenium phases are present on the surface: metallic rhenium and a heavily reducible rhenium phase that interacts strongly with the support [17]. Several studies of bimetallic reforming catalysts (Pt–Re) conclude that rhenium and platinum form alloyed metal particles [18,19].

Based on this information, we have used *in situ* X-ray absorption spectroscopy to study the bimetallic interaction and the metal–support interaction in rhenium-promoted cobalt Fischer–Tropsch catalysts. Co–Re/Al_2O_3 catalysts for Fischer–Tropsch synthesis usually have high cobalt loading (10–20 wt%) and low rhenium loading (ca. 1 wt%). The EXAFS signal from the rhenium absorption edges is hampered by absorption and scattering due to the large amount of cobalt and from the support. Samples containing 4.6 wt% cobalt and 2 wt% rhenium were used in order to minimise this problem. The relatively high rhenium loading made it possible to perform the experiments in transmission mode. We have previously shown that approximately 0.8 wt% of cobalt in this sample is present as metallic cobalt [13]. The rest, 3.8 wt%, is randomly distributed as Co(II) in the vacant sites in the defect alumina spinel lattice. The contribution to the overall EXAFS signal from cobalt metal is not significant enough to yield information about any bimetallic interactions. In the present study, the nature of rhenium has been studied for different reduction periods for rhenium-promoted Fischer–Tropsch synthesis catalysts supported on alumina.

2. Experimental

2.1. Catalyst preparation

Catalysts containing 4.6 wt% cobalt and 2 wt% rhenium supported on γ-Al_2O_3 were prepared by incipient wetness

* To whom correspondence should be addressed.

coimpregnation of the support with aqueous solutions of $Co(NO_3)_2{\cdot}6H_2O$ and $HReO_4$. The catalysts were dried in air overnight at 120 °C and calcined for 2 h at 400 °C. A catalyst containing 2 wt% rhenium on the same support was made using the same procedure.

2.2. XAS measurements

Transmission XAS data were collected at the Swiss–Norwegian Beamline (SNBL) at the European Synchrotron Radiation Facility (ESRF), France. Spectra were obtained at the rhenium L_{III} edge (10 535 eV) using a channel-cut Si(111) monochromator. Higher order harmonics were rejected by means of a chromium-coated mirror angled at 3.5 mrad with respect to the beam to give a cut-off energy of approximately 14 keV. The beam currents ranged from 130–200 mA at 6.0 GeV. The maximum resolution ($\Delta E/E$) of the Si(111) bandpass is 1.4×10^{-4} using a beam of size 0.6 × 7.2 mm. Ion chamber detectors with their gases at ambient temperature and pressure were used for measuring the intensities of the incident (I_0) and transmitted (I_t) X-rays. The detector gases were as follows: I_0, detector length 17 cm, 100% N_2; I_t, length 31 cm, 35% Ar, 65% N_2.

The amounts of material in the samples were calculated from element mass fractions and the absorption coefficients of the constituent elements [20] just above the absorption edge to give an absorber optical thickness close to 1.5 absorption lengths. The samples were ground and sieved (7–125 μm) and mixed with the requisite amount of boron nitride to achieve the desired absorber thickness. The samples were then loaded into a Lytle *in situ* reactor-cell [21] and reduced in a mixture of H_2 (5%) in helium (purity 99.995%, flow rate 60 ml/min) by heating at a rate of 4 °C/min from room temperature to 450 °C and maintaining that temperature for 1–12 h (see table 1). Four to eight scans were taken and summed for each sample. The energy calibration was checked by measuring the spectrum of a rhenium foil (thickness 0.0125 mm) with the energy of the first inflection point being defined as the edge energy.

2.3. EXAFS data analysis

The data were corrected for dark currents, converted to k-space, summed and background subtracted to yield the EXAFS function $\chi(k)$ using the *EXCALIB* and *EXBACK* programs [22]. Model fitting was carried out with *EXCURV90* using curved-wave theory and *ab initio* phase shifts [22,23]. During the least squares fitting it is important to minimise correlation effects between the parameters that strongly affect the EXAFS amplitude and those that influence the frequency of the EXAFS oscillations. Therefore, the EXAFS data were least squares fitted in k space using k^0- and k^3-weighted data. Coupling between N (multiplicity) and $2\sigma^2$ (Debye–Waller-type factors) was reduced by choosing solutions common to both weighting schemes [24]. The k^3 weighting scheme compensates for the diminishing photoelectron wave at higher k values. Low k weighting enhances the contribution from lighter backscattering atoms such as oxygen, thereby allowing metal–support interactions to be included in the analysis. By carrying out this procedure on appropriate reference compounds as well as for the unknown spectra, more accurate coordination numbers can be obtained than what otherwise is the case [19,25–27]. As an indication on the quality of the fit, the residual index, R_χ (%) is defined as

$$R_\chi = \frac{\sum_i [(\chi_i^{\mathrm{exp}} - \chi^{\mathrm{calc}})k^{\mathrm{WT}}]^2}{\sum_i [\chi_i^{\mathrm{exp}})k^{\mathrm{WT}}]^2} \times 100\%.$$

A rhenium metal foil (0.0125 mm), ReO_3 and $(NH_4)ReO_4$ (both the solid salt and an aqueous solution containing ReO_4^-) were used as model compounds to check the validity of the *ab initio* phase shifts and establish the general parameters AFAC (amplitude reduction factor) and VPI (accounts for inelastic scattering of the photoelectron) [22]. Due to the lack of sufficient models for the Re–Co distances, the theoretical phase shifts and amplitude factors for this backscatterer has not been checked. The validity of the parameters associated with the Re–Co contribution is therefore uncertain. Structural parameters of the reference compounds [28–30] are listed in table 2.

3. Results

Figure 1 compares the rhenium L_{III} EXAFS spectra of the bimetallic catalyst for different reduction periods. The EXAFS spectra of the sample containing only rhenium on alumina are shown in figure 2. The parameters obtained

Table 1
Details concerning the Re L_{III} EXAFS analysis.

Sample	Reduction period at 450 °C	Data range Δk (Å^{-1})	Quality of fit[a] (%)
4.6% Co–2% Re/Al_2O_3	Before reduction	3.5–11	13.1
4.6% Co–2% Re/Al_2O_3	1 h	3.5–12	22.2
4.6% Co–2% Re/Al_2O_3	6 h	3.5–12	20.0
4.6% Co–2% Re/Al_2O_3	12 h	3.5–12	20.9
2% Re/Al_2O_3	Before reduction	3.5–12	11.9
2% Re/Al_2O_3	6 h	3.5–12	25.7

[a] Defined in the text.

Table 2
Crystallographic data for the EXAFS model compounds used to check the validity of the *ab initio* phase shifts and backscattering amplitudes.

Compound	Model pair	R^a (Å)	N^b	Reference
Re foil	Re–Re	2.74	12	[27]
$(NH_4)ReO_4$	Re–O	1.74	4	[28]
ReO_3	Re–O	1.87	6	[29]

[a] Interatomic distance.
[b] Coordination number (multiplicity).

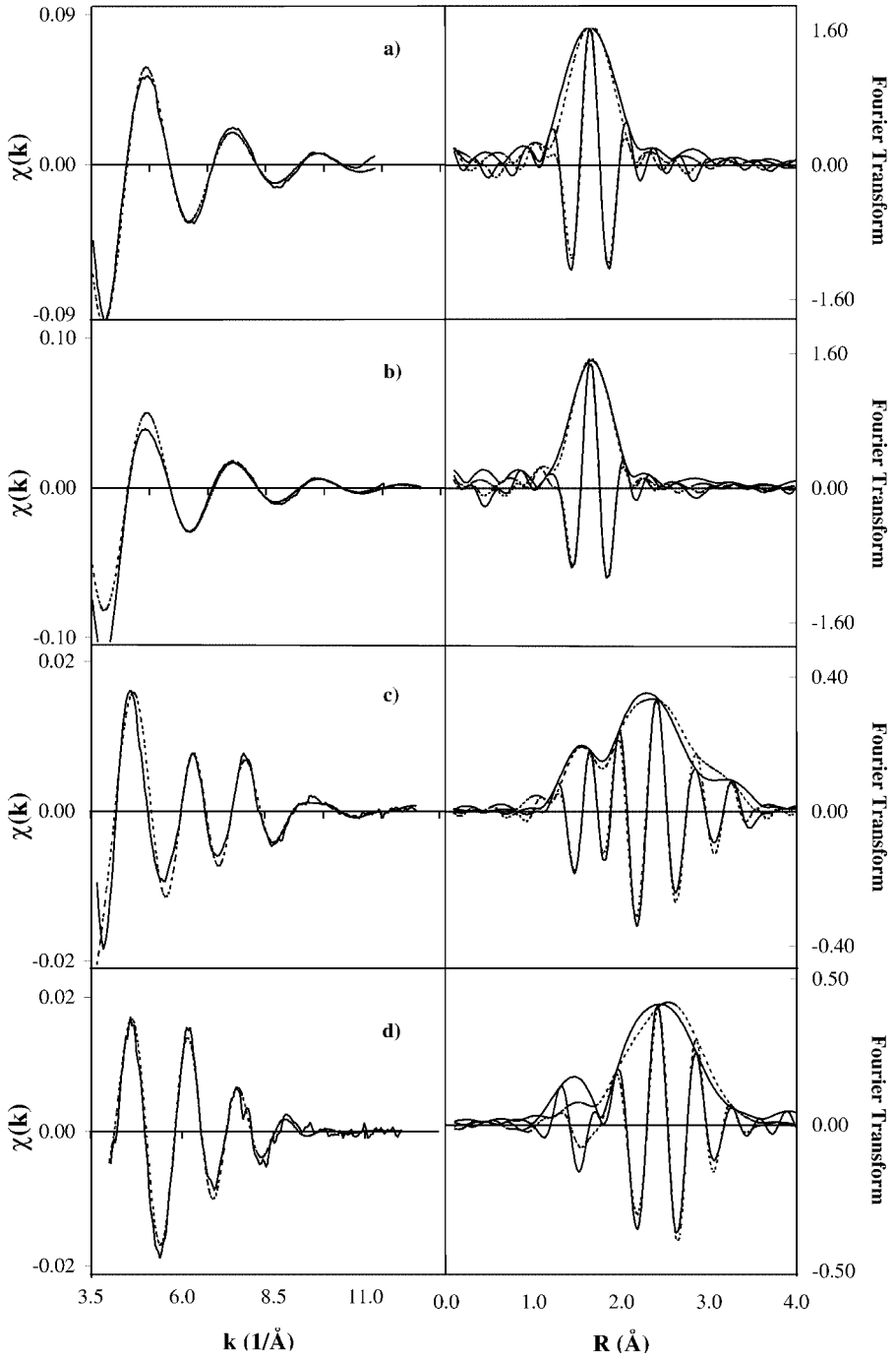

Figure 1. Re L_{III} EXAFS spectra (left) and the corresponding Fourier transforms (right) of the bimetallic catalyst containing 2 wt% Re and 4.6 wt% Co on Al_2O_3: (a) before reduction, (b) reduced for 1 h at 450 °C, (c) reduced for 6 h at 450 °C and (d) reduced for 12 h at 450 °C. The spectra are Fourier filtered using a wide window of 1.0–25.0 Å (i.e., no noise removal). Experiment is shown in solid lines, and k^0 fit in dotted lines.

from the EXAFS analysis are summarised in table 3 for the bimetallic catalyst and in table 4 for the monometallic counterpart.

Before reduction, the EXAFS from both the bimetallic (Co–Re/Al_2O_3) and the monometallic (Re/Al_2O_3) samples are modelled by a single Re–O coordination shell only. The coordination numbers and interatomic distances are identical to that of ReO_4^-. This is also the case for the bimetallic catalyst sample reduced for 1 h at 450 °C. Although the Re–O coordination is reduced from 4.0 to 3.4 after reduction for 1 h, no metal–metal coordination could be detected at this stage.

For the samples reduced 6 and 12 h, four shells had to be included in the model to give acceptable agreement with the experimental data. The EXAFS of the bimetallic catalyst contains contributions from two Re–O distances and two Re–metal distances. The two Re–O contributions arise from interaction with oxygen in the support and from unreduced

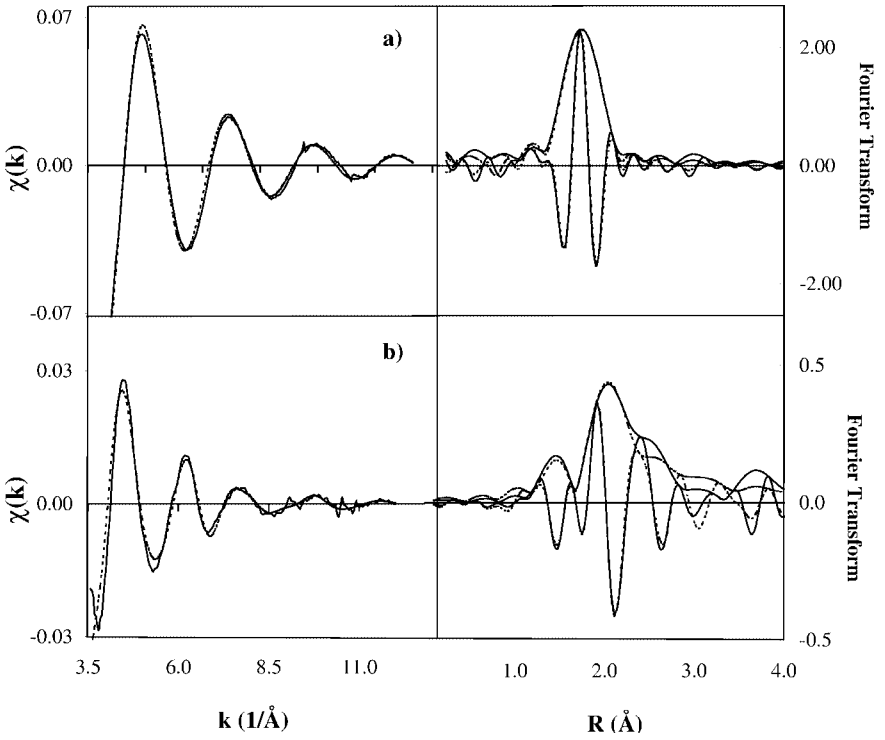

Figure 2. Re L_{III} EXAFS spectra (left) and the corresponding Fourier transforms (right) of the bimetallic catalyst containing 2 wt% Re on Al_2O_3: (a) before reduction and (b) reduced for 6 h at 450 °C. The spectra are Fourier filtered using a wide window of 1.0–25.0 Å (i.e., no noise removal). Experiment is shown in solid lines, and k^0 fit in dotted lines.

Table 3
Results from the EXAFS analysis of data from the Re L_{III} edge of the sample containing 4.6% Co–2% Re/Al_2O_3.[a]

Reduction at 450 °C	Coordination shell	E_0 (eV)	N	$2\sigma^2$ (Å^2)	R (Å)
No reduction	Re–O	15.1(2)	4.0(1)	0.006(1)	1.74(1)
1 h	Re–O	15.1(3)	3.4(1)	0.006(1)	1.74(1)
6 h	Re–O	13.0(3)	0.7(1)	0.003(1)	1.74(1)
	$Re–O_{support}$		1.7(2)	0.020(2)	2.00(1)
	Re–Co		2.1(2)	0.022(2)	2.53(2)
	Re–Re		2.4(3)	0.016(2)	2.71(2)
12 h	Re–O	13.3(3)	0.2(1)	0.002(0)	1.76(1)
	$Re–O_{support}$		1.4(1)	0.018(2)	1.99(1)
	Re–Co		3.2(1)	0.024(2)	2.54(1)
	Re–Re		4.0(3)	0.024(2)	2.69(1)

[a] Each bonding distance (R) is associated with a coordination number (N) and thermal vibration and static disorder (Debye–Waller-like factor, $2\sigma^2$). E_0 is the refined correction to the threshold energy of the absorption edge. The standard deviation in the least significant digit as calculated by *EXCURV90* is given in parentheses. However, note that such estimates of precision (which reflect statistical errors in the fitting) overestimate the accuracy, particularly in cases of high correlation between parameters. The estimated standard deviations for the distances are 0.01–0.02 Å, with ±20% accuracy for N and $2\sigma^2$. Although the accuracy for these is increased by refinements using k^0 vs. k^3 weighting [24].

rhenium (present as rhenium oxide). The Re–metal interactions are best modelled by including both rhenium and cobalt contributions. A significant contribution from a second rhenium shell is detected in the spectrum from the Re/Al_2O_3 sample that is reduced for 6 h. The second Re–Re contribution is therefore included in the fit.

Table 4
Results from the EXAFS analysis of data from the Re L_{III} edge of the sample containing 2% Re/Al_2O_3.[a]

Reduction at 450 °C	Coordination shell	E_0 (eV)	N	$2\sigma^2$ (Å^2)	R (Å)
No reduction	Re–O	16.4(3)	4	0.003(0)	1.74(1)
6 h	Re–O	18.7(4)	0.6(1)	0.004(0)	1.74(1)
	$Re–O_{support}$		2.4(2)	0.017(2)	1.98(1)
	Re–Re		5.1(2)	0.035(4)	2.67(2)
	Re–Re		3.0(2)	0.030(3)	3.65(2)

[a] See footnote to table 3.

4. Discussion

Rhenium in the unreduced catalysts and in the bimetallic catalyst reduced for 1 h at 450 °C is clearly present as ReO_4^-. A small fraction of the rhenium in the samples reduced for 6 h is still in the Re^{+VII} oxidised state represented by the Re–O distance at 1.74 Å. The Re^{+VII} oxide contribution is negligible in the catalyst reduced for 12 h at 450 °C. The Re–O distance is slightly longer for this sample (1.76 Å), indicating that the rhenium atoms in the oxide may be partially reduced to a lower oxidation state.

The EXAFS results confirm that bimetallic particles are formed in the catalyst. The metal particles in the catalyst reduced for 6 h at 450 °C contain on average approximately 50% cobalt and 50% rhenium (coordination numbers 2.1 and 2.4, respectively). When reduced for 12 h, the Re–Re coordination is raised to 4.0 and the cobalt coordination to 3.2. Higher coordination numbers are evidence of larger metal

particles, indicating that sintering takes place during prolonged reduction periods. This is also reflected in the rhenium enrichment of the particles in the sample reduced for 12 h. In contrast, the Fischer–Tropsch catalyst containing 0.14 wt% ruthenium and 11.6 wt% cobalt on TiO_2 [8] contained particles where ruthenium was coordinated to approximately twelve metal atoms after reduction. The large difference in size between rhenium and ruthenium particles is most likely due to the easier reducibility of ruthenium compared to rhenium.

We have previously shown that the amount of unreduced cobalt in the catalyst constitutes 3–4 wt% of the sample material [13]. This fraction of cobalt atoms diffuses into the vacant sites in the defect spinel lattice of the alumina support. In the same study, we also showed that the remaining cobalt is reduced to metal already after 15 min. The metal–support interaction is, in the present study, shown to be significant for rhenium as well. The monometallic sample (table 4) exhibits a pronounced Re–O interaction at ca. 2.0 Å which is associated with the interaction between rhenium and oxygen in the support material [19]. The metal–support interaction is weaker in the bimetallic catalyst (table 3) which is reflected in lower $Re–O_{support}$ coordination numbers than for the monometallic sample. This may be due to the alumina spinel lattice being saturated with cobalt [13] and therefore not so easily accessible by rhenium atoms.

The results presented in table 3 show that rhenium is not reduced after 1 h at 450 °C. Even after reduction for 6 h about 20% of the rhenium is present as rhenium oxide. Extending the reduction period to 12 h results in almost complete reduction of the rhenium oxide, except for the rhenium phase that is closely bound to the support. It is believed that rhenium promotes the reduction of cobalt [31,32]. Our results are consistent with this suggestion since rhenium is reduced at a later stage than cobalt in the reduction sequence. This is confirmed by the presence of bimetallic particles in the catalyst, which may be formed by mobile rhenium oxide species migrating over the surface. The mobility allows for intimate contact with cobalt and hence formation of alloyed particles.

An interesting observation is that cobalt does not seem to catalyse the reduction of rhenium in the same manner as observed for the reduction of rhenium in platinum–rhenium catalysts [18,33]. The amount of reduced rhenium is practically the same in the monometallic and the bimetallic samples. Furthermore, the metal particles seem to be of the same size in the monometallic sample as in the bimetallic. Both samples have first-shell Re–metal coordination close to 5.0. The introduction of cobalt does, however, seem to alter the morphology of the metal particles, since a second Re–metal coordination sphere can only be detected in the monometallic sample. The second-shell contribution is found at 3.65 Å and contains an average of three rhenium atoms (see table 4). This contribution is absent in the bimetallic catalyst. This is probably due to a larger degree of disorder in the bimetallic particles leading to a large number of backscattering contributions at different distances. Consequently, none of these contributions is large enough to be detected in the overall spectra.

The Re–Re distances in the reduced samples are found to be ca. 2.70 Å. This is shorter than the Re–Re distances in bulk rhenium metal (2.74 Å). From the EXAFS analysis, the Re–Co distances are determined to be ca. 2.54 Å. This is slightly longer than the Co–Co distances found in bulk cobalt metal (2.49 Å) [13] and considerably shorter than the Re–Re distances. Note, however, the uncertain reliability of the Re–Co interaction since no appropriate model compound was available to check the validity of the calculated phase shifts. Contractions of interatomic distances in metal clusters have been reported earlier as an indication of small particles [13,34,35]. Based on the observed average coordination numbers [34] and the contracted Re–Re distances, we conclude that the average particle sizes are less than 15 Å for the reduced samples.

5. Conclusion

X-ray absorption spectroscopy of the Re L_{III} absorption edge confirms bimetallic particle formation in $Co–Re/Al_2O_3$ catalysts after reduction at 450 °C. The metal particles in the sample with 4.6 wt% cobalt and 2 wt% rhenium contain approximately equal amounts of the two elements when reduced for 6 h. The average particle size is less than 15 Å. Reduction for 12 h causes sintering of the particles, forming larger particles of different composition. The rhenium metal particles in Re/Al_2O_3 are of the same size as the bimetallic particles in the $Co–Re/Al_2O_3$ sample.

The monometallic sample exhibits stronger metal–support interactions than the bimetallic sample. Cobalt atoms randomly distributed over the vacant tetrahedral sites in the alumina support partially obstruct rhenium atoms from accessing these sites. Rhenium is not reduced after 1 h of hydrogen exposure at 450 °C. The reduction of rhenium therefore occurs subsequent to the reduction of cobalt. After 6 h reduction, ca. 80% of the rhenium is completely reduced in the monometallic sample as well as in the bimetallic counterpart, suggesting that the reduction of rhenium is not catalysed by cobalt. Further reduction of the bimetallic catalyst (12 h) leads to the complete reduction of rhenium, except for the rhenium phase that interacts strongly with the support.

Acknowledgement

The authors thank the Research Council of Norway for support and acknowledge the staff at the Swiss–Norwegian Beam Lines (SNBL) at the ESRF for their assistance (Experiment No. 01-01-97).

References

[1] H. Schulz, Appl. Catal. A 186 (1999) 3.
[2] J.J.C. Geerlings, J.H. Wilson, G.J. Kramer, H.P.C.E. Kuipers, A. Hoek and H.M. Huisman, Appl. Catal. A 186 (1999) 27.

[3] S. Eri and J.G. Goodwin, US Patent 4 857 599 (1989).
[4] S. Eri, J.G. Goodwin and T. Riis, US Patent 4 801 573 (1989).
[5] S. Eri, J.G. Goodwin and T. Riis, US Patent 4 880 763 (1989).
[6] Y. Borodko and G.A. Somorjai, Appl. Catal. A 186 (1999) 355.
[7] E. Iglesia, Appl. Catal. A 161 (1997) 59.
[8] E. Iglesia, S.L. Soled, R.A. Fiato and G.H. Via, J. Catal. 143 (1993) 345.
[9] G.P. Huffman, N. Shah, J. Zhao, F.E. Huggins, T.E. Hoost, S. Halvorsen and J.G. Goodwin, Jr., J. Catal. 151 (1995) 17.
[10] B. Ernst, A. Bensaddik, L. Hilaire, P. Chaumette and A. Kiennemann, Catal. Today 39 (1998) 329.
[11] L. Chin and D.M. Hercules, J. Phys. Chem. 86 (1982) 360.
[12] D. Schanke, A.M. Hilmen, E. Bergene, K. Kinnari, E. Rytter, E. Ådnanes and A. Holmen, Catal. Lett. 34 (1995) 269.
[13] A. Moen, D.G. Nicholson, M. Rønning and H. Emerich, J. Mater. Chem. 8 (1998) 2533.
[14] F.B. Noronha, M. Schmal, R. Frety, G. Bergeret and B. Moraweck, J. Catal. 186 (1999) 20.
[15] Z. Zsoldos and L. Guczi, J. Phys. Chem. 96 (1992) 9393.
[16] B. Moraweck, R. Frety, G. Pecchi, M. Morales and P. Reyes, Catal. Lett. 43 (1997) 85.
[17] H.C. Yao and M. Shelef, J. Catal. 44 (1976) 392.
[18] R. Prestvik, B. Tøtdal, C.E. Lyman and A. Holmen, J. Catal. 176 (1998) 246.
[19] A.S. Fung, M.J. Kelley, D.C. Koningsberger and B.C. Gates, J. Am. Chem. Soc. 119 (1997) 5877.
[20] *International Tables for X-ray Crystallography*, Vol. 3 (Kynoch Press, Birmingham, 1962) p. 175.
[21] F.W. Lytle, R.B. Greegor, E.C. Marques, D.R. Sandstrom, G.H. Via and J.H. Sinfelt, J. Catal. 95 (1985) 546.
[22] N. Binsted, J.W. Campbell, S.J. Gurman and P.C. Stephenson, *EXCALIB, EXBACK* and *EXCURV90* programs, SERC Daresbury Laboratory (1990).
[23] S.J. Gurman, N. Binsted and I. Ross, J. Phys. C 17 (1984) 143.
[24] F.W.H. Kampers, C.W.R. Engelen, J.H.C. van Hooff and D.C. Koningsberger, J. Phys. Chem. 94 (1990) 8574.
[25] D.C. Koningsberger and R. Prins, ed. *X-ray Absorption: Principles, Applications, Techniques of EXAFS, SEXAFS and XANES* (Wiley, New York, 1988).
[26] F.W. Lytle, D.E. Sayers and E.A. Stern, eds., Physica B 158 (1989) 701;
S.S. Hasnain, ed., *X-ray Absorption Fine Structure* (Hellis Horwood, Chichester, 1991).
[27] M. Vaarkamp, Catal. Today 39 (1998) 271.
[28] *International Tables of X-ray Crystallography*, Vol. 3 (Kynock Press, Birmingham, 1962) p. 281.
[29] R.J.C. Brown, S.L. Segel and G. Dolling, Acta Crystallogr. B 36 (1980) 2195.
[30] K. Meisel, Z. Anorg. Allg. Chem. 207 (1932) 121.
[31] S. Vada, A. Hoff, E. Ådnanes, D. Schanke and A. Holmen, Topics Catal. 2 (1995) 155.
[32] D. Schanke, S. Vada, E.A. Blekkan, A.M. Hilmen, A. Hoff and A. Holmen, J. Catal. 155 (1995) 85.
[33] S.M. Augustine and W.M.H. Sachtler, J. Catal. 116 (1989) 184.
[34] B.J. Kip, F.B.M. Duivenvoorden, D.C. Koningsberger and R. Prins, J. Catal. 105 (1987) 26.
[35] B.S. Clausen, H. Topsøe, L.B. Hansen, P. Stolze and J.K. Nørskov, J. Catal. 114 (1994) 463.